High efficiency *pin* waveguide photodetectors

ABID KARIM
Iqra University, Defence View, Shaheed-e-Millat Road (Ext.), Karachi, Pakistan

A waveguide photodetector (WGPD) is very attractive device for future optical communication systems and optoelectronic integrated circuits (OEIC) because the wide bandwidth operation at higher quantum efficiencies can be obtained. Also, these devices have advantage of packaging technology, since waveguide structure, which is similar to laser structure, is suitable for planar OEIC. Furthermore, it can be operated under zero-bias and biased conditions. In this paper, the performance of zero-bias and biased *pin* waveguide photodetector is compared with respect to internal quantum efficiency and internal quantum efficiencies as high as 105% are achieved.

1. Introduction

The demand in speed and capacity of information processing is increasing day by day. Optical communication systems will be required to have a high capacity of information processing and transmission. Therefore, optoelectronic devices or circuits used in communication systems must keep the pace with these requirements or be developed even further. One of the most important optoelectronic components in a typical optical fiber network is a photodetector as it ultimately limits the overall system performance [1]. A waveguide photodetector shares the same operating mechanism with that of conventional photodetector, however, the active waveguide optical detector has several advantages over the conventional photodetector such as:

1. High speed response can be achieved at zero bias [2] because the direction of incident radiation and carrier collection are normal to each other.

2. WGPD is illuminated from side rather than from top (which is the case in a conventional photodetector). This increases detection efficiency as photons are absorbed along the length of the device [3].

3. Zero bias operation not only offers circuit simplicity but also makes the dark current noise negligible which help to improve the signal to noise ratio [4,5].

4. These detectors have a structure which is similar to a laser and hence they are relatively easy to integrate into complex OEICs.

Although, a WGPD can be operated under zero-bias condition [6], however, the performance of WGPD can be enhanced by operating it under bias conditions.

2. Quantum effieciency of WGPD

The internal quantum efficiency, η_{in} of a WGPD under reverse bias or zero bias conditions, can be calculated as [7]:

$$\eta_{in} = \frac{S_{in}hc}{e\lambda}\left(1 - \frac{\alpha_o}{\alpha_o + \Gamma\alpha_{ib}}\right) \qquad (1)$$

where S_{in} is the internal or actual sensitivity of WGPD, c is the speed of light in vacuum, h is the Plank's constant, λ is the wavelength of the incident radiation, e is the charge on an electron, α_o represents the residual waveguide absorption losses and α_{ib} is the interband absorption. S_{in} can be given as [8]:

$$S_{in} = \frac{S_{ext}}{\zeta(1-R)} \qquad (2)$$

here S_{ext} is the external sensitivity of the detector, ζ is the coupling efficiency of optical radiation and R is the facet reflectivity. S_{ext} can be defined as:

$$S_{ext} = \frac{\eta_{ext}e\lambda}{hc} \qquad (3)$$

and the coupling efficiency can be calculated as [9]:

$$\zeta = \frac{\eta_{ext}}{(1-R)(1-e^{-\Gamma\alpha_{ib}L})} \qquad (4)$$

3. Experimental procedure

In order to compare the performance of a zero-bias WGPD and a biased WGPD, two stripe geometry A. R. coated laser like devices were used. A 5 *um* wide stripe laser diode (LD) was used as the source laser throughout the work reported in this paper. Structural parameters of the various devices used during the work reported in this paper are listed in table-1. All device were essentially made from the same GaAs/AlGaAs material and for these devices, α_o

was measured as 24/cm using the conventional cutback loss measurement technique [10]. The length of all devices was 250 um. This length was quite sufficient for complete absorption of optical radiation coming from the source.

Table 1. Structural parameter of different devices used during the work reported here.

Device number	Stripe width, W (μm)	Active layer thickness (μm)	R$_1$ (%)	R$_2$ (%)
1	2.5	0.15	4	4
2	5	0.15	4	4
3 (Source laser)	5	0.15	30	30

All the devices were mounted on separate copper heat sink blocks. Temperatures of the device being tested and of the source laser were controlled independently using thermoelectric Peltier devices and a multi-channel temperature controller. Throughout the work reported in this paper, the test devices were subjected to pulsed input from the source laser which was operated under pulse conditions using a HP8082A pulse generator to avoid overheating in order to achieve more reliable results. The width of current pulses was kept constant at 200ns with a repetition frequency of 10 kHz. This proportion between the pulse width and pulse repetition frequency was sufficient to isolate the transient temperature effects caused by one pulse from other pulses [11]. Along with an optical lens system, a pre-calibrated large area Si detector (LAD) and WGPD (being investigated) were used to measure light output. An infrared camera was used for alignment of LD and WGPD as and when required. The source laser and WGPD were aligned using a free-space alignment technique [12]. Results were plotted using a Tektronix sample & hold oscilloscope and an X-Y plotter.

4. Results and discussion

4.1 Response of WGPD

After achieving the maximum alignment between the source laser and WGPD, the response of WGPD was analyzed by measuring I-L characteristic of the source laser using the device-1 as a WGPD and a pre-calibrated large area photodetector (LAD). Results of both measurements are shown in Fig. 1. It can be seen from Fig. 1 that the response of a pre-calibrated Si LAD and the GaAs WGPD are similar to each other except the sensitivity. This indicates that there was a perfect alignment between the source laser and WGPD.
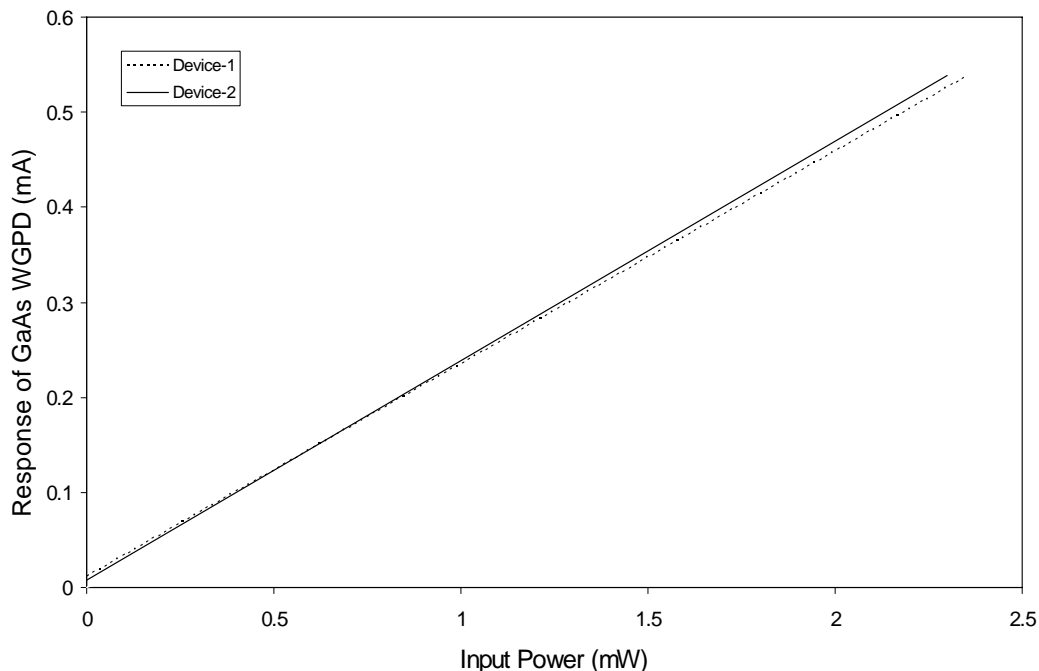

Fig. 2. Response of WGPDs as a function of stripe width.

The same experimental procedure was repeated using a 5μm wide stripe device (device-2) instead of device-1 as a WGPD. The response of both WGPDs (i.e. device 1 & 2) as a function of stripe width is plotted in Fig. 2. It can be seen from Fig. 2 that the change in the stripe width does not have much effect on the response of GaAs WGPD. This was expected because the minimum achieved spot size was smaller than the stripe width of 2.5μm [6]. From Fig. 2, the

external sensitivity, S_{ext} of GaAs WGPD was calculated as around 0.22A/W. This value does satisfy the reported values of refs. 9 & 13. Using eq. (3), the external quantum efficiency was estimated as 31. 8%. For the typical values of η_{ext} = 31.8%, $R_1 = R_2$ = 4%, L = 250 μm and Γ = 46% [6],

α_{ib}= 200/cm [8], ζ was calculated as 35.26% and S_{in} was calculated as 0.63 A/W. Finally, η_{in} for the devices being investigated was estimated as around 72% by substituting all required values in eq. (1).
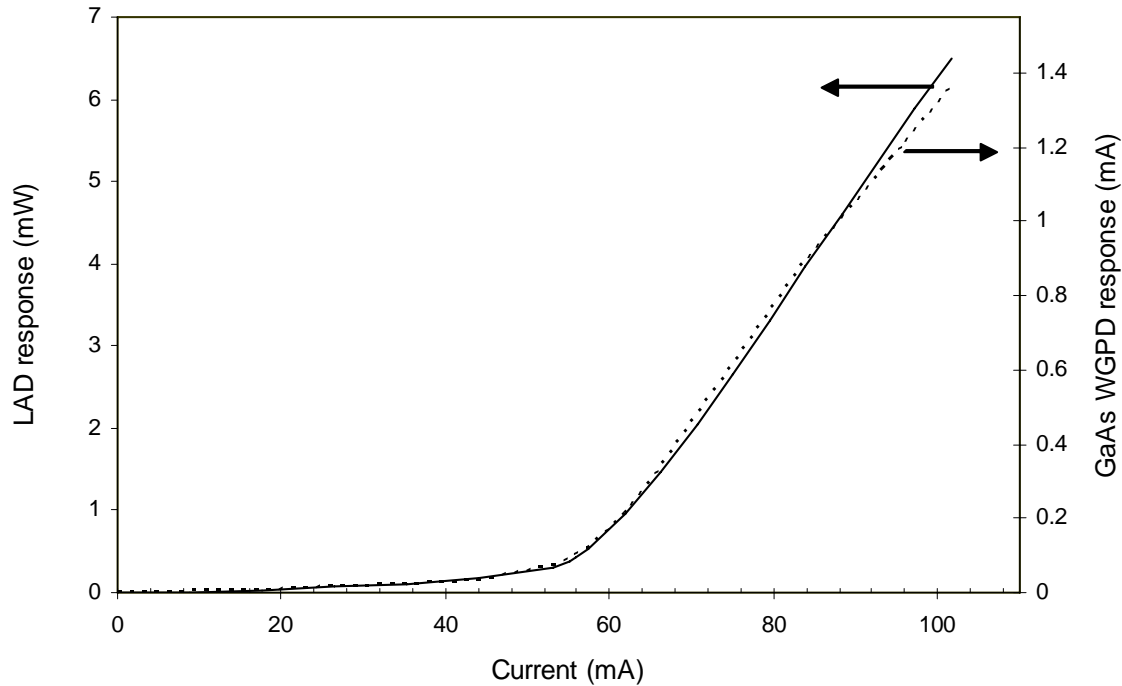

Fig. 1. I-L characteristics of the source laser measured using LAD and GaAs WGPD.

4.2 Effect of biasing on the response of WGPD

The effect of biasing on the performance of WGPD was investigated by applying a variable reverse bias voltage to WGPDs (device-1) while it was subjected to a pulsed input power from the source laser. As the bias voltage to the WGPD was increased, the output of the WGPD was increased till reaching a maximum or saturation value. Similar effects were observed for device-2 as well. This type of behavior was expected because photons from the source laser are absorbed in the active layer of the WGPD and generate electron-hole pairs. Generated electrons and holes decay to the bottom of the conduction band and to the top of the valence band. If the intraband relaxation time is much larger than the interband relaxation time, as is usually the case for an optically pumped lasers, a population may build-up, which is further increased by the charge trapping at the potential barrier (which is meant to confine the carrier within the active layer). When an external electric field is applied, the trapped holes surmount the potential well easily and interband relaxation overcomes the intraband band relaxation time due to the increase in the mobility of minority carriers [14]. As the reverse bias voltage increases, the height of depletion barrier increases, which results in an increase in absorption coefficient [15].

In order to evaluate quantum efficiencies (i.e. internal and external quantum efficiencies) of the WGPD as a function of the reverse bias voltage, external and internal sensitivities of GaAs WGPDs calculated at different levels of reverse bias voltage. From internal and external sensitivity figures, internal and external quantum efficiencies were calculated and are plotted in Fig. 3. Both types of efficiencies of the GaAs WGPD reach 90% of their maximum value at around -0.8V of the bias voltage. This corresponds to the height of the potential well [16] and it is close to the reported value of -0.82V [17].
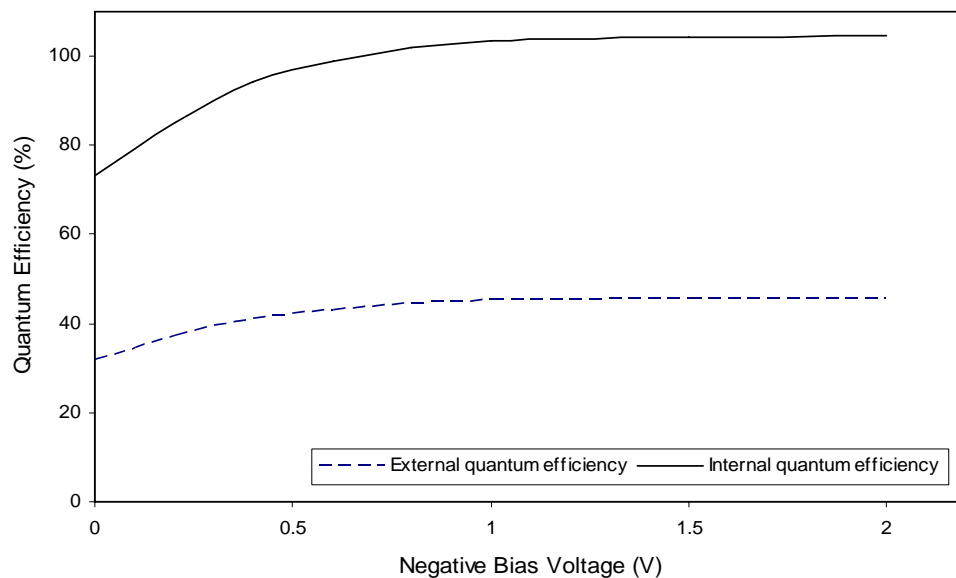
Fig. 3. Graph showing a significant difference between η_{in} and η_{ext} of GaAs WGPD.

5. Conclusions

In conclusion we can say that a WGPD with thick absorption or active layer has higher η_{ext}. However, η_{ext} is the external conversion efficiency and it does not represent the internal conversion efficiency of the device. Hence increase in active layer thickness does not affect the internal quantum efficiency. η_{in} of WGPDs made from the same material with different active layer thickness would be more or less same provided incoming light is fully decayed in waveguide.

In this paper, the effect of biasing on quantum efficiencies is examined experimentally. It was found that in zero-bias WGPD saturation takes place due to charge trapping at potential barrier, which is meant for carrier confinement. Under the influence of external applied field, charge trapping can be avoided. Also with reverse biasing, the height of depletion barrier increases, thus resulting in higher absorption coefficient. As a result of higher absorption coefficient, internal quantum efficiency as high as 105% is obtained. This highest reported value of detection for a *pin* type WGPDs.

References

[1] Nikoufard, L. Xu, X. J. M Leijtens, T. de Vries, E. Smalbrugge, R. Nötzel, Y. S. Oei, M. K. Smit, Proceedings of 14th European conference on integrated optics, Eindhoven, Netherlands, 143, 2008.
[2] J. E. Bowers, C. A. Burrus, F. Mitschke, Electron. Lett. **22**, 633 (1986).
[3] J. E. Bowers, C. A. Burrus, Electron. Lett. **22**, 905 (1986).
[4] M. Erman, Ph. Riglet, Ph. Jarry, B. G. Martin, M. Renaud, J. F. Vinchant, J. A. Cavailles, IEE Proc. 138, Part-J, 101, 1991.
[5] J. Alping, R. Tell, S. T. Eng, J. of Lightwave Tech. **LT-4**, 1662 (1986).
[6] A. Karim, J. of Microelectronics, Electronic Components and Materials **39**(3), 125 (2009).
[7] Larsson, P. A. Andrekson, S. T. Eng, A. Yariv, IEEE J. Quantum Electron. **QE-24**, 787 (1988).
[8] D. Moss, D. Landheer, D. Conn, D. Halliday, S. Charbonneau, G. Aers, R. Barber, F. Chatenoud, IEEE Photonics Tech. Lett. **4**, 609 (1992).
[9] J. Alping, IEE Proc. **136-J**, 177 (1989).
[10] E. Pinkas, B. I. Miller, I. Hayashi, P. W. Foy, IEEE J. of Quantum Electron. **QE-9**, 281 (1973).
[11] A. Karim, The Arabian Journal of Science & Tech. **22**, 75 (1997).
[12] A. Karim, Semiconductor Physics, Quantum Electronics and Optoelectronics **5**, 319 (2002).
[13] Sasaki, M. Nishiuma, Y. Takeda, Jap. J. of Applied Phys. **9**, 1695 (1980).
[14] B. E. A. Saleh, M. C. Teich, Fundamental of photonics, John Wiley, 1991.
[15] M. J. Sun, K. H. Nichols, W. S. C. Chang, R. O. Gregory, F. J. Rosenbaum, C. M. Wolfe, Applied Optics **17**, 1568 (1978).
[16] J. E. Bowers, C. A. Burrus, J. of Lightwave Tech. **LT-5**, 1339 (1987).
[17] R. D. Baertsch, J. R. Richardson, J. of Appl. Phys. **40**, 229 (1969).

_____
*Corresponding author : akarimpk@iqra.edu.pk
akarimpk@yahoo.com